Title	On-chip microwave photonic system through multi-component micro-transfer print integration
Authors	Atar, Fatih Bilge;Arafat, Yeasir;Mishra, Darpan;O'Callaghan, James;Piwonski, Tomasz;Waqas, Abi;Moynihan, Owen;Dominguez, Diego;Roycroft, Brendan;Gunning, Fatima;Thomas, Kevin;Pelucchi, Emanuele;Corbett, Brian
Publication date	2024-11-04
Original Citation	Atar, F. B., Arafat, Y., Mishra, D., O'Callaghan, J., Piwonski, T., Waqas, A., Moynihan, O., Dominguez, D., Roycroft, B., Gunning, F., Thomas, K., Pelucchi, E. and Corbett, B. (2024) 'On-chip microwave photonic system through multi-component micro-transfer print integration', 2024 International Topical Meeting on Microwave Photonics (MWP), Pisa, Italy, 17-20 September 2024, pp. 1-4. https://doi.org/10.1109/MWP62612.2024.10736314
Type of publication	Conference item
Link to publisher's version	10.1109/MWP62612.2024.10736314
Rights	© 2024, IEEE. Personal use of this material is permitted. Permission from IEEE must be obtained for all other uses, in any current or future media, including reprinting/republishing this material for advertising or promotional purposes, creating new collective works, for resale or redistribution to servers or lists, or reuse of any copyrighted component of this work in other works.
Download date	2025-12-05 20:57:12
Item downloaded from	https://hdl.handle.net/10468/16728

University College Cork, Ireland
Coláiste na hOllscoile Corcaigh

On-chip Microwave Photonic System through Multi-component Micro-transfer Print Integration

Fatih Bilge Atar[1], Yeasir Arafat[1], Darpan Mishra[1], James O'Callaghan[1], Tomasz Piwonski[1], Abi Waqas[1], Owen Moynihan[1], Diego Dominguez[1], Brendan Roycroft[1], Fatima Gunning[1], Kevin Thomas[1], Emanuele Pelucchi[1], Brian Corbett[1]

[1]Tyndall National Institute, University College Cork, Cork Ireland T12 R5CP
e-mail: fatih.atar@tyndall.ie

***Abstract*— We demonstrated a photonic integrated circuit (PIC) with heterogeneously integrated InP-based lasers and uni-travelling carrier photodiodes (UTC-PD) for microwave photonics applications. The InP components are integrated via the micro-transfer printing (MTP) technique, which allows scalable manufacturing process of the microwave photonic chips. We used the photonic circuit to form an external cavity with the transfer printed laser device and achieved tunable single frequency lasing for use in heterodyne radio frequency (RF) generation. The heterogeneously integrated UTC-PDs had 80 GHz bandwidth, and we validated RF generation on UTC-PD with the emission from an on-chip laser.**

Keywords—integrated microwave photonics, heterogeneous integration, micro-transfer printing

I. Introduction

Microwave photonics (MWP) deals with converting RF (radio frequency) data between electronic and optical domains, and processing RF signals in the optical domain by using a photonic circuit [1]. Microwave systems have now access to the abundant bandwidth at optical frequencies and to flexible design topologies thanks to reconfigurable photonic circuits [2]. MWP has proven itself as a viable technology to address the increasing bandwidth requirements of telecommunication technologies while achieving the low noise levels required by advanced modulation schemes [3]. Chip-scale integration of MWP components aim to address the fundamental problems of traditional systems, which are high power consumption and bulky instrumentation, and advance the microwave technology to higher data throughput at lower SWAP (size, weight and power consumption) [1]. There have been numerous reports on various microwave processing functions on photonic chips [4, 5], establishing reconfigurable photonic circuit platforms [2, 6] and maturing integrated photonics platforms to realize MWP chips [4, 7-8].

The current technology relies on flip-chip bonding, die-attach or fiber-attach to introduce laser light to the photonic chips, which are serial processes that limit the manufacturing throughput. Heterogeneous integration techniques, such as wafer bonding and micro-transfer printing, has started to prove their potential to enable mass-manufacturing of photonic chips with high-performance active components [9-12].

In this paper, we report for the first time a self-contained microwave photonic chip enabled by multi-component micro-transfer print integration. As a proof-of-concept demonstration, the photonic chip generates optical frequency lines with the on-chip laser and converts them to microwave signal on the high-speed photodetector heterogeneously integrated on the same chip (Fig. 1(a)). Here we discuss the design principles and the integration interfaces, explain the chip fabrication process and report on the component characterization measurements.

II. Photonic Chip Design

A. Components for Heterogeneous Integration

We designed InP based separate confinement heterostructure laser devices and uni-travelling carrier photodiodes (UTC-PD) for micro-transfer print integration on SiN photonic integrated circuit. UTC-PD requires small dimensions in order to keep the capacitance to a minimum for high-speed operation, which necessitates coupling from a tightly confined waveguide. A laser, on the other hand, either requires carefully engineered evanescent coupling structures or edge-coupling to large waveguides, due to its relatively large-spot size. In this study we demonstrated an often overlooked advantage of MTP, which is the ability to integrate different coupling interfaces on the same PIC as required by the device properties (Fig. 1(b)). For the laser, we followed the edge coupling approach and engineered an SU-8/SiN spot-size converter (Fig. 1(c, d)). The dimensions of SU-8 waveguide were chosen to achieve high mode overlap with the laser. The simulated modal area of the laser structure is 3 μm^2 with a 2.5 µm rib waveguide. The simulated overlap of the laser mode with the mode of 0.8 µm thick and 2 µm wide SU-8 waveguide is 90%. The light is evanescently coupled from the SU-8 waveguide into the 400 nm thick SiN waveguide through a tapered waveguide structure. UTC-PDs were printed on 1 µm wide SiN waveguides with a thin (< 50 nm) adhesive layer and the light was coupled evanescently into the InP/InGaAs layers. We used Lumerical MODE and Lumerical FDTD software for the simulations of the modal properties, mode overlaps, tapered spot size converter and the coupling / absorption in the UTC-PD. Fig. 2 shows the epitaxial structures of the laser and UTC-PD, and the mode profiles of

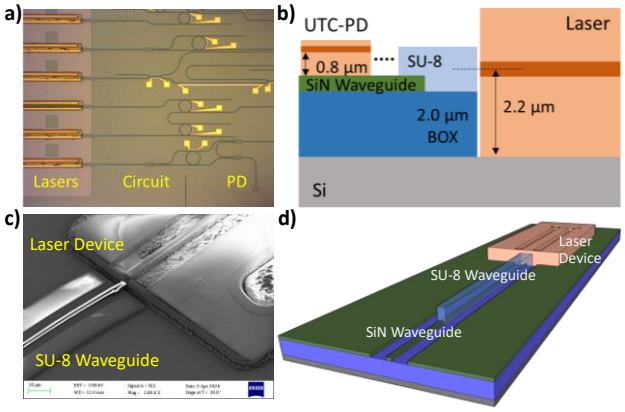

Fig. 1. (a) Optical microscope image of fabricated PIC with on-chip lasers and UTC-PD. (b) Schematic cross-section showing the vertical alignment of the waveguides and the active devices on the PIC. (c) SEM image showing the front facet of the laser device and the SU-8 waveguide. (d) Schematic drawing of the SU-8/SiN spot size converter that edge couples the light from the laser.

This research is funded by Enterprise Ireland Disruptive Technologies Innovation Fund Project DT/2019/0080 TAPESTRY, Science Foundation Ireland (12/RC/2276_P2) and Horizon Europe research and innovation programme under the Marie Skłodowska-Curie Grant Agreement 101073138 (MWP4SPACE).

the laser with this epitaxial structure and the matching SU-8 waveguide.

Both devices are grown with the same AlInAs / InGaAs release layer [12]. The laser has a multi-quantum well gain stack between asymmetric waveguiding layers. The thickness of the n-InP layer is chosen to match the mode height of the laser to the SiN waveguide when the laser is printed on Si substrate (with SiO_2 layer fully etched) to avoid additional thermal resistance between the laser and the Si substrate.

We simulated the electrical properties of the UTC-PD in Silvaco ATLAS. Within the practical limits, most layer thicknesses are kept to minimum to achieve a small device resistance. The absorber layer needs to be thick enough to efficiently absorb the evanescently coupled light within a very small device length (5-10 µm) while maintaining a small transit time of photogenerated charge carriers and a small device resistance. Similarly, due to the requirement of incorporating a partial etching of the n-contact layer in the fabrication process (to avoid placing the n-metal on the collector, which would compromise the contact resistivity), we used a relatively thick n-contact layer to maintain low lateral resistance between the n-metal and the active device area. The trade-off is a slight increase in the vertical device resistance and reduced evanescent optical coupling to the absorber layer from the underlying SiN waveguide. For a device length of 10 µm, Lumerical FDTD simulations could achieve up to 70% absorption, which depended heavily on the device geometry including the thicknesses of the coatings and the adhesive layer.

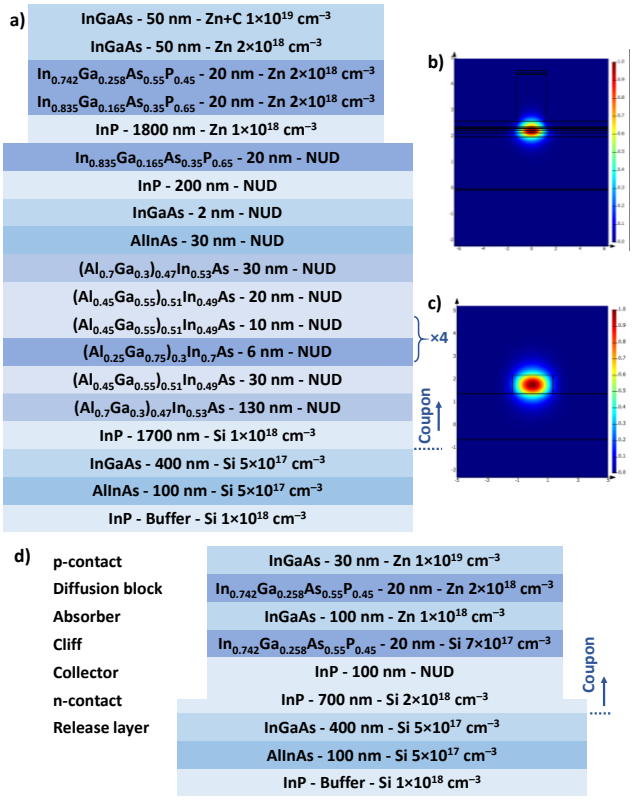

Fig. 2. (a) Epitaxial structure of the laser device. (b) E-field profile of the TE mode of the laser. (c) E-field profile of the SU-8 waveguide that is designed to give high overlap with the laser. (d) Epitaxial structure of the UTC-PD.

B. *Microwave Frequency Generator Photonic Circuit*

We designed photonic circuits to obtain tunable, single frequency emission from on-chip lasers, two of which could be combined on the UTC-PD for heterodyne microwave frequency generation (Fig. 3(a)). The photonic circuit was designed to feedback the overlapping resonance wavelength of two Vernier tuned ring resonators (r_1 = 50 µm, r_2 = 54 µm) to achieve single frequency operation in an extended cavity laser configuration (Fig. 3(b)). Additionally, we designed another configuration to demonstrate RF generation with micro-transfer printed laser and UTC-PD on the same SiN PIC platform (400 nm SiN on 2 µm SiO_2). No SiO_2 over-cladding was used to reduce the fabrication complexity but the full fabrication process is compatible for the deposition and patterning of the over-cladding layer. End-fire coupled output ports of the SiN PICs were made with SU-8 waveguides (with tapered spot-size converters similar to the ones used for edge-coupling from the transfer printed lasers as shown in Fig. 1) to increase the mode diameter of the output ports. A lensed fiber was used to capture the emission from the end-fire output ports of the PIC for optical power and optical spectrum measurements.

For the bandwidth characterization of UTC-PDs, we fabricated separate test platforms on SOI platform (220 nm Si on 2 µm SiO_2). The PIC had pairs of grating couplers connected to each other. We transfer printed UTC-PDs on the grating couplers on one side, and used the grating couplers on the other side to couple modulated laser light into the chip through a cleaved fiber.

III. Characterization

A. *Single Frequency Lasing*

Figure 4(a) and Fig. 4(b) show the lasing spectra obtained from the PIC with transfer printed laser coupon and double ring Vernier filter. The shift of the lasing wavelength with the voltage applied to the microheaters adjacent to the ring resonators is also visible in the lasing spectra.

In this photonic circuit, the lasing wavelength is ideally tuned by the simultaneous control of both heaters to adjust the lasing peak to the desired wavelength. As seen in the spectra of Fig. 4 the lasing peak could be tuned by applying voltage to only one heater, which should have caused the lasing peak

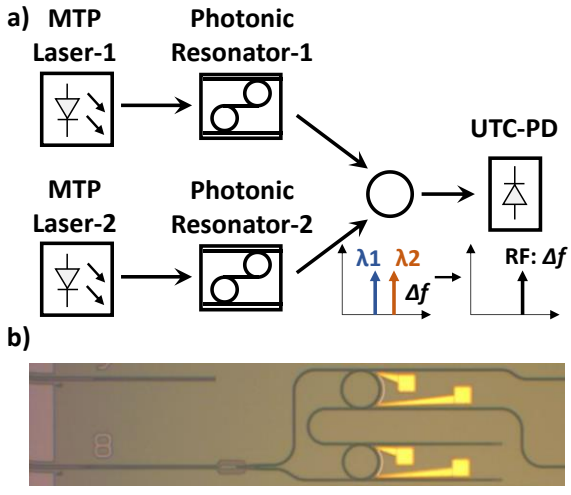

Fig. 3. (a) Schematic diagram of the microwave frequency generator PIC investigated in this study. (b) Optical microscope image of the Vernier tuned ring resonator circuit.

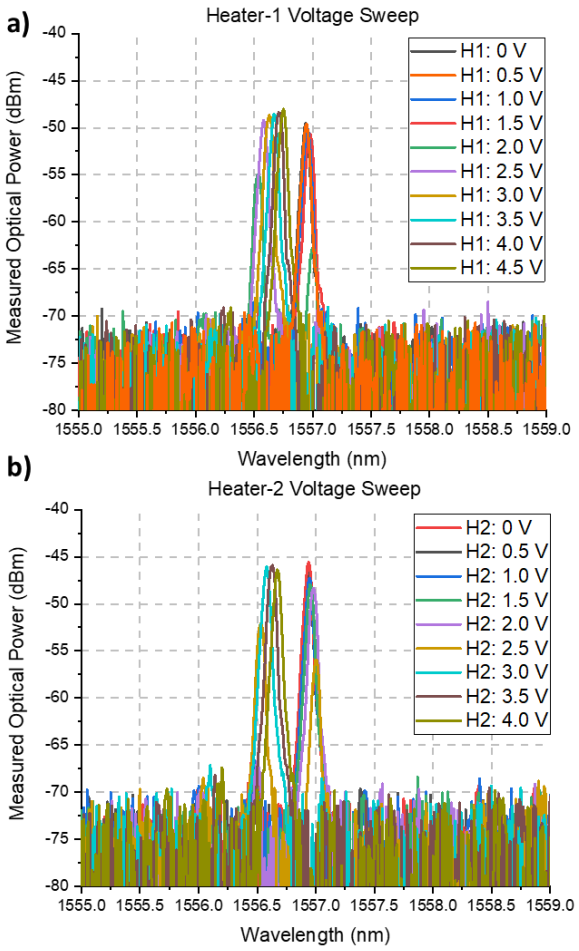

Fig. 4. (a, b). Lasing spectra measured from the on-chip laser with different bias voltages applied to Heater-1 and Heater-2, respectively.

to disappear or jump to the next overlapping wavelength in a photonic circuit with high-Q resonators. The observed results indicate that the ring resonators are over-coupled in this PIC fabrication. This unintended feature allows us to tune the lasing wavelength with a single microheater but we expect the optical power is mostly trapped in the external cavity and the linewidth improvement with ring resonators is not present. The measurement with simultaneous tuning of both ring resonators could not be carried out due to the limitations of the experimental setup.

B. UTC-PD Bandwidth and Heterodyne RF Generation

We carried out the bandwidth measurements of UTC-PDs on 220 nm SOI platform by using grating couplers. Anritsu MS 4647B 110 GHz Optical Vector Network Analyzer (OVNA) was used for the measurements. Laser light (1550.116 nm wavelength, 6.98 dBm optical output power) was modulated with Port 1 output of OVNA and a half-wave plate was used to adjust the polarization of the laser light before coupling it to the PIC through a grating coupler. Port 2 was connected to the UTC-PDs through a V-cable, bias-T (65 GHz) and RF probes (65 GHz, GSG). Prior to the measurement of UTC-PDs, an Anritsu 110 GHZ calibrated photodiode was used to get the reference spectrum and to correct for the response of the bias-T and V-cable that were used in the measurement setup. We plotted the S21 measurement results for UTC-PDs with different device dimensions in Fig. 5(a). We note that the response of the GSG probes and contact pads are also included in the measured bandwidth. The smallest device (Width: 2.5 µm, Length: 5.0 µm) has a 3 dB frequency of 42 GHz and 6 dB frequency of 80 GHz.

With the same test sample and a similar experimental setup, we validated heterodyne frequency generation on UTC-PDs (Fig. 5(b)). Two external laser sources were polarized independently so that they could be combined on the grating coupler with the same polarization (passing through 2×1 combiner, EDFA and bandpass filter). The wavelength of one of the lasers was tuned to obtain a heterodyne signal on the UTC-PD in the 5 GHz - 50 GHz range. The electrical spectra were measured with Agilent 8565EC Spectrum Analyzer (30 Hz – 50 GHz).

C. Multi-component Integration for Frequency Generation

On the SiN platform, we fabricated a PIC to demonstrate RF generation on the transfer printed UTC-PD with the light generated by a transfer printed laser on the same PIC. A schematic drawing of the PIC is shown in Fig. 6(a). The SiN photonic circuit has a ring resonator that feeds the resonance wavelengths of the ring back to the laser device to create an external cavity and obtain single frequency lasing. One of the through ports of the ring resonator is connected to the UTC-PD and the other one is connected to an output port of the PIC. The output port is also connected to UTC-PD through 1x2

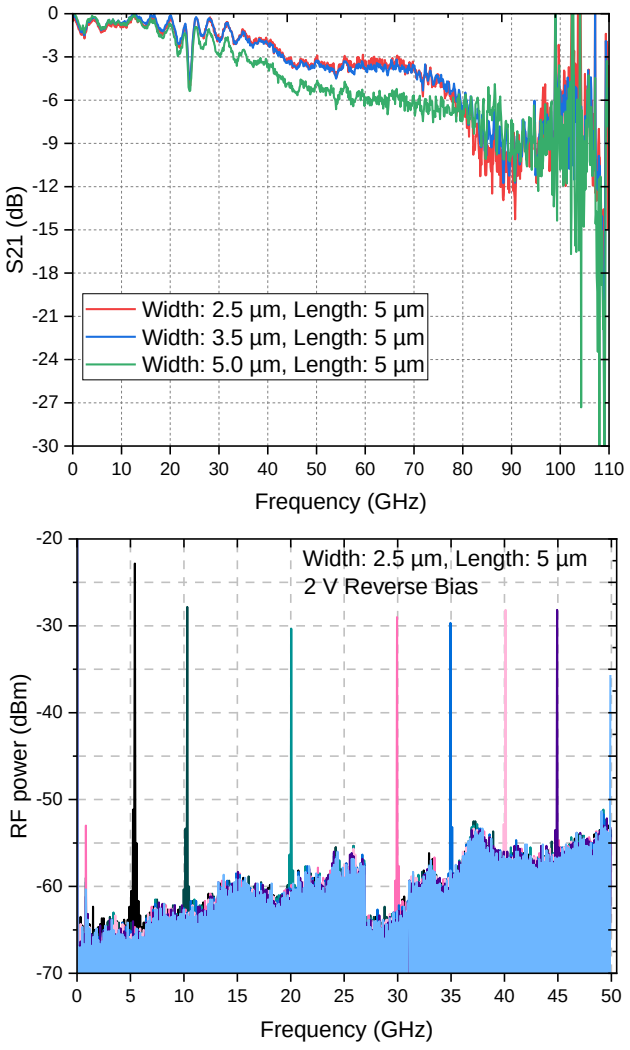

Fig. 5. (a) Bandwidth measurement of UTC-PDs with different device dimensions. (b) Electrical spectra of Heterodyne RF signal generation experiment on UTC-PD (Width: 2.5 µm, Length: 5.0 µm).

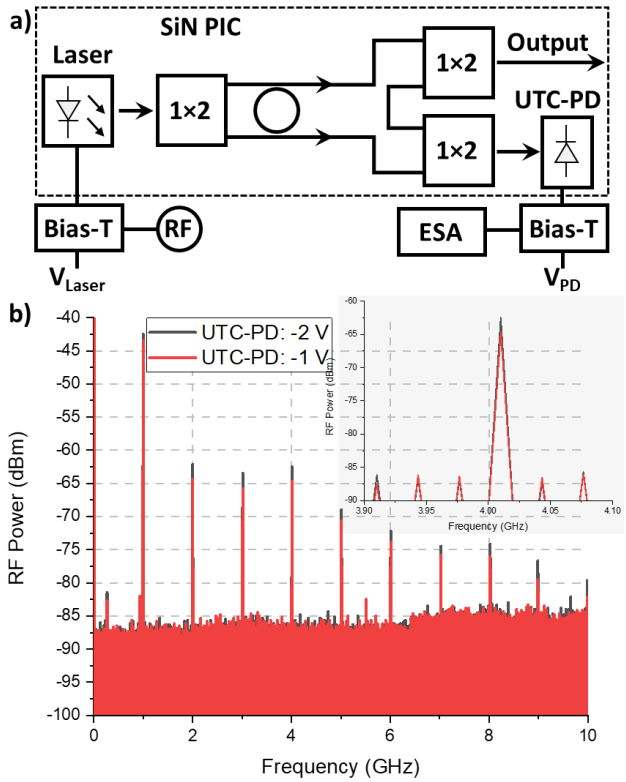

Fig. 6. (a) Schematic diagram of the demonstrator PIC and the measurement configuration. (b) Electrical spectra measured from the UTC-PD under 1 V and 2 V reverse bias. Spectra show the harmonics of the gain switching frequency (1 GHz) applied to the laser on the same PIC. The inset is a close up on the peak at 4 GHz. The RF response increased by 2.5 dB with the increasing reverse bias voltage.

MMI (multi-mode interference) couplers for testing purposes. The laser device is gain switched with 1-2 GHz frequencies to generate optical frequency lines at the harmonics of the drive frequency. Harmonics up to 10 GHz were measured from the UTC-PD on the same PIC with Agilent 8565EC Spectrum Analyzer (Fig. 6(b)). Increasing the reverse bias from 1 V to 2 V increased the RF response by 2.5 dB.

IV. Conclusion and Future Work

On our photonic integration platform, we demonstrated the joint operation of two InP based devices with very different photonic interfaces, namely laser and UTC-PD. Without the need for an external laser source, we showed RF generation on the UTC-PD by gain switching the on-chip laser to obtain the harmonics of the drive frequency. A heterodyne generation PIC was designed, which would eliminate the need for RF drive and allow better flexibility in RF generation. We validated the viability of the designed heterodyne RF generation PIC by measuring the tunable single frequency operation of the lasers and high-speed operation of the UTC-PD. Fabrication of the complete heterodyne RF generation PIC on a low-loss photonic integration platform with high-Q ring resonators remains as the next step to obtain narrow linewidth lasers, and achieve tunable & low-noise RF generation. Other important directions for research are detailed analysis of the coupling between InP components and the SiN waveguides for edge coupling and evanescent coupling schemes, investigation of different laser designs for high-power and low-noise operation, and a thorough study of the linearity and responsivity of the UTC-PD designs and their trade-off with coupling efficiency from the PIC. Advanced packaging of the PIC with high-speed electronics is another research challenge for the operation at microwave and mm-wave bands.

Acknowledgment

The authors would like to acknowledge Shengtai Shi and Frank Peters from the Integrated Photonics Group, and Shivangi Chugh, Cleitus Antony and Paul Townsend from Photonics Systems Group at Tyndall National Institute for their help and support for the bandwidth measurements of UTC-PDs.

References

[1] D. Marpaung, J. Yao, and J. Capmany, "Integrated microwave photonics." Nature photonics 13.2 (2019): 80-90.

[2] Z. Tao, et al. "Highly reconfigurable silicon integrated microwave photonic filter towards next-generation wireless communication." Photonics Research 11.5 (2023): 682-694.

[3] O. Daulay, G. Liu, X. Guo, M. Eijkel, D. Marpaung, "A tutorial on integrated microwave photonic spectral shaping." Journal of lightwave technology 39.3 (2021): 700-711.

[4] Y. Liu, D. Marpaung, A. Choudhary, J. Hotten, B. J. Eggleton, "Link performance optimization of chip-based Si3N4 microwave photonic filters." Journal of Lightwave Technology 36.19 (2018): 4361-4370.

[5] M. Reza, et al. "Design and performance estimation of a photonic integrated beamforming receiver for scan-on-receive synthetic aperture radar." Journal of Lightwave Technology 39.24 (2021): 7588-7599. C. Porzi, M. Reza, P. Ghelfi, M. Sorel, A. Bogoni, "Silicon-on-insulator microwave photonic filter with widely tunable and reconfigurable flat-top bandpass functionality." Journal of Lightwave Technology 40.20 (2022): 6666-6675.

[6] Y. Liu, Y. Yu, L. Wang, Y. Yu, X. Zhang, "Reconfigurable Microwave Photonic Bandpass Filter Based on CROW." Journal of Lightwave Technology (2023).

[7] S. Iezekiel, M. Burla, J. Klamkin, D. Marpaung, J. Capmany, "RF engineering meets optoelectronics: Progress in integrated microwave photonics." IEEE Microwave Magazine 16.8 (2015): 28-45.

[8] Y. Liu, A. Choudhary, D. Marpaung, B. J. Eggleton, "Integrated microwave photonic filters." Advances in Optics and Photonics 12.2 (2020): 485-555.

[9] C. Xiang, et al. "High-performance silicon photonics using heterogeneous integration." IEEE Journal of Selected Topics in Quantum Electronics 28.3: Hybrid Integration for Silicon Photonics (2021): 1-15.

[10] P. Kaur, et al. "Hybrid and heterogeneous photonic integration." APL Photonics 6.6 (2021).

[11] B. Haq, et al. "Micro-transfer-printed III-V-on-silicon C-band distributed feedback lasers." Optics Express 28.22 (2020): 32793-32801.

[12] H. Muthuganesan, et al. "100 Gbps PAM4 ultra-thin photodetectors integrated on SOI platform by micro transfer printing." Optics Express 31.22 (2023): 36273-36280.